Polylactide Toughening with Epoxy-Functionalized Grafted Acrylonitrile–Butadiene–Styrene Particles

Shulin Sun,[1] Mingyao Zhang,[1] Huixuan Zhang,[1] Xiumei Zhang[2]

[1]*Engineering Research Center of Synthetic Resin and Special Fiber (Ministry of Education), Changchun University of Technology, Changchun 130012, China*
[2]*First Hospital of Jilin University, Changchun 130021, China*

Received 18 August 2010; accepted 29 December 2010
DOI 10.1002/app.34111
Published online 6 July 2011 in Wiley Online Library (wileyonlinelibrary.com).

ABSTRACT: Glycidyl methacrylate functionalized acrylonitrile–butadiene–styrene (ABS-*g*-GMA) particles were prepared and used to toughen polylactide (PLA). The characteristic absorption at 1728 cm^{-1} of the Fourier transform infrared spectra indicated that glycidyl methacrylate (GMA) was grafted onto the polybutadiene phase of acrylonitrile–butadiene–styrene (ABS). Chemical reactions analysis indicated that compatibilization and crosslinking reactions took place simultaneously between the epoxy groups of ABS-*g*-GMA and the end carboxyl or hydroxyl groups of PLA and that the increase of GMA content improved the reaction degree. Scanning electron microscopy results showed that 1 wt % GMA was sufficient to satisfy the compatibilization and that ABS-*g*-GMA particles with 1 wt % GMA dispersed in PLA uniformly. A further increase of GMA content induced the agglomeration of ABS-*g*-GMA particles because of crosslinking reactions. Dynamic mechanical analysis testing showed that the miscibility between PLA and ABS improved with the introduction of GMA onto ABS particles because of compatibilization reactions. The storage modulus decreased for the PLA blends with increasing GMA content. The decrease in the storage modulus was due to the chemical reactions in the PLA/ABS-*g*-GMA blends, which improved the viscosity and decreased the crystallization of PLA. A notched impact strength of 540 J/m was achieved for the PLA/ABS-*g*-GMA blend with 1 wt % GMA, which was 27 times than the impact strength of pure PLA, and a further increase in the GMA content in the ABS-*g*-GMA particles was not beneficial to the toughness improvement. © 2011 Wiley Periodicals, Inc. J Appl Polym Sci 122: 2992–2999, 2011

Key words: blending; core–shell polymers; compatibilization; toughness

INTRODUCTION

The toughening of polylactide (PLA) has been investigated in recent years, and most studies have focused on biocompatible materials. The toughening methodologies have included copolymerization strategies,[1–3] plasticization with a miscible component,[4–7] and blending with an immiscible homopolymer or a block copolymer.[8–21] However, the improvement of the toughness was very limited with these strategies.

The toughness of PLA can be improved by the incorporation of a rubbery phase. However, simple blending of PLA with other components usually cannot produce satisfactory properties because of the unfavorable interaction between molecular segments of the components, which is responsible for their immiscibility or poor interfacial adhesion. To improve the miscibility of polymer blends and increase the interfacial adhesion between the matrix and disperse phases, reactive compatibilization is very often used to obtain blends with desirable properties. This method is based on the formation of a block or grafted A–B copolymer at the interface between the blend phases during melt mixing. The A–B copolymers can increase the interfacial strengths and reduce the droplet coalescence rates through steric repulsion.[22–24]

Because most polymer blends do not have the appropriate functional groups, functionalization of the components is very often required.[25–27] Fortunately, the inherent chemical functionality of PLA makes it an attractive candidate for modification. Some authors have described approaches for improving the toughness of PLA by the reaction of a polymer containing an appropriate chemical functionality with the carboxyl or hydroxyl end groups of PLA during melt processing. Functionalized elastomers, such as poly(ethylene-*co*-glycidyl methacrylate) (EGMA), have been used to toughen PLA.[28] The epoxy group of glycidyl methacrylate (GMA) can react *in situ* with the carboxyl and hydroxyl end groups of PLA during melt blending and can lead to

Correspondence to: X. Zhang (zhangxiumei1959@163.com).
Contract grant sponsor: National Natural Science Foundation of China; contract grant number: 50803007.
Contract grant sponsor: Jilin Provincial Science and Technology Department; contract grant number: 20090142.

an EGMA-grafted PLA copolymer that can compatibilize the blend. Other rubbers containing GMA, such as glycidyl methacrylate grafted poly(ethylene octane) (POE-*g*-GMA) have also been used to toughen PLA by the same mechanism.[29]

Core–shell impact modifiers, such as acrylonitrile–butadiene–styrene (ABS), are another important type of toughener of PLA. Li and Shimizu[30] explored the use of a reactive styrene–acrylonitrile–glycidyl methacrylate (SAN–GMA) copolymer as a compatibilizer for PLA/ABS blends. This SAN–GMA copolymer contained reactive epoxy groups, which could react with PLA end groups (—COOH or —OH) under melt conditions and form a copolymer of PLA and styrene–acrylonitrile (SAN). So, the interfacial tension decreased between PLA and ABS, and the toughness of PLA is improved.

In this study, we explored another option for compatibilizing PLA/ABS blends. In this study, glycidyl methacrylate functionalized acrylonitrile–butadiene–styrene (ABS-*g*-GMA) core–shell particles were prepared in an emulsion polymerization process. During the synthesis of ABS, different contents of GMA monomer were added to the reactive system, so ABS particles with different epoxy group contents were obtained. Compared with PLA/compatibilizer/ABS blends, ABS-*g*-GMA was more suitable for the toughening of PLA. First, the functionalization of the impact modifier was carried out during the preparation process of ABS, so this method was simpler. Second, the GMA was grafted onto the shell phase of ABS, which was located in the interface between ABS and PLA, so the interfacial reactions between the two phases were much easier. In this study, the polymerization properties of GMA, the influence of GMA content on the chemical reactions, and the rheological, morphological, and mechanical properties of the PLA/ABS blends were studied in detail.

EXPERIMENTAL

Materials and preparation

The PLA was purchased from Biomaterial, Ltd. (Ningbo Huanqiu, China). The molecular weight and molecular weight distribution of PLA were 220,000 and 1.6, respectively. The ABS and ABS-*g*-GMA materials were synthesized by an emulsion polymerization method in our laboratory, and the properties are listed in Table I. The particle sizes of ABS and ABS-*g*-GMA were measured by a Brookhaven particle size analyzer (Holtsville, NY), and the torque measurements were performed on a Thermo Haake mixer (Karlsruhe, Germany). The rotating speed was set at 50 rpm, and the temperature was set at 180°C.

Fourier transform infrared (FTIR) analysis

FTIR was used to analyze the grafting properties of GMA during the preparation process of ABS-*g*-GMA. The ABS-*g*-GMA copolymer was dissolved in acetone, and the solution was ultracentrifuged at room temperature at 10,000 rpm with a GL-21M ultracentrifuge (Shanghai Centrifuge Institute Co., Ltd., Shanghai, China). After 30 min, clear separation was achieved. The ungrafted SAN and/or SAN-*co*-GMA were soluble in acetone, whereas the ABS and/or ABS-*g*-GMA copolymer were insoluble. The insoluble part was concentrated in a white layer at the tube bottom, and the clear solution of the ungrafted copolymer was concentrated at the top of the tube; this part was used for FTIR analysis.

Blending and molding procedures

The blending of the PLA/ABS-*g*-GMA blends was performed on a Thermo Haake mixer. The weight percentage of ABS or ABS-*g*-GMA in the PLA blends was 30 wt %. The rotating speed was set at 50 rpm, and the temperature was set at 180°C. The mixing time was 5 min. The blends were then compression-molded for 5 min at 180°C to form 4-mm thick specimens for notched Izod impact testing.

Dynamic mechanical analysis (DMA)

The dynamic mechanical properties of the PLA blends were characterized with DMA. The measurements were carried out on a Diamond dynamic mechanical analyzer (Selb, Germany). The scans were carried out in tensile mode. The samples were $30 \times 10 \times 1$ mm^3, and the test was carried out in the temperature range 20–160°C at a frequency of 10 Hz and a heating rate of 3°C/min.

TABLE I
Properties of ABS and ABS-*g*-GMA

Designation	Rubber content (wt %)	AN/St ratio (wt/wt)	GMA content (wt %)	Particle size (μm)	Torque (Nm)
ABS	60	25/75	0	0.40	25.8
ABS-*g*-GMA1	60	25/75	1	0.41	25.6
ABS-*g*-GMA3	60	25/75	3	0.43	25.7
ABS-*g*-GMA5	60	25/75	5	0.42	25.8
ABS-*g*-GMA7	60	25/75	7	0.42	25.6

Morphological properties

The disperse morphology of ABS and ABS-*g*-GMA in the blends was characterized by scanning electron microscopy (SEM; model Japan JSM-5600, JEOL Ltd., Tokyo, Japan). The blend samples were frozen in liquid nitrogen for 2 h and then fractured in brittle mode. Then, the samples were coated with a gold layer for SEM observation.

Mechanical properties

The notched Izod impact strength of PLA blends were measured by an XJU-22 Izod impact tester (Chengde Tester Machinery Factory, Chengde, China) at 23°C according to ASTM D 256. The tensile tests were carried out with an AGS-H tensile tester (Shimadzu Corporation, Kyoto, Japan) at a crosshead speed of 50 mm/min at room temperature according to ASTM D 638.

RESULTS AND DISCUSSION

FTIR analysis

Figure 1 shows the FTIR spectra of the ABS and ABS-*g*-GMA copolymers with different GMA contents. For a comparison, the peak at 1728 cm^{-1} was the strong carbonyl group characteristic absorption of GMA, which indicated that the GMA monomer was introduced onto the ABS copolymer. At the same time, it could be found that the absorbance intensity of carbonyl groups increased with the increase of GMA content in the ABS-*g*-GMA copolymers.

The ABS-*g*-GMA7 copolymer sample was selected for analyzing the grafting properties of GMA on the ABS particles. The experimental method was described in the Experimental section. The FTIR spectra of the insoluble fraction (graft copolymer) and the soluble fraction (free copolymer) of the ABS-*g*-GMA7 copolymer extracted from acetone are shown in Figure 2. Both curves showed the characteristic absorption of GMA at 1727 cm^{-1}, which indicated that part of the GMA monomers grafted onto the polybutadiene (PB) particles or copolymerized with styrene (St) and acrylonitrile (AN) in the grafting shell and part of the GMA monomers copolymerized with St and AN to form free SAN-*co*-GMA copolymers.

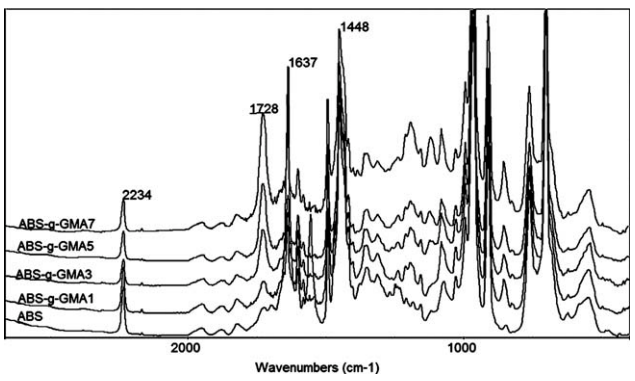

Figure 1 FTIR spectra of ABS and the ABS-*g*-GMA copolymers.

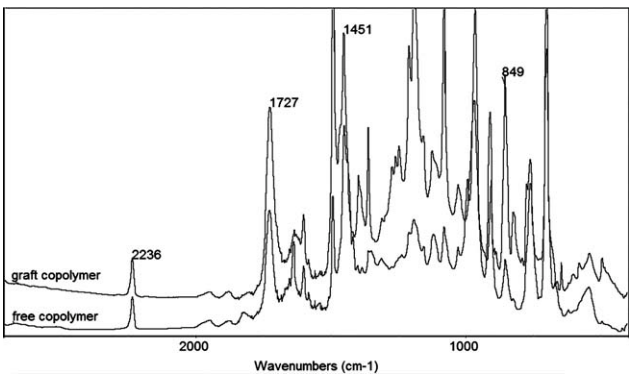

Figure 2 FTIR spectra of an ABS-*g*-GMA copolymer separated with acetone.

Chemical reaction analysis

Two kinds of reactions may take place between the carboxyl or hydroxyl end groups of PLA and the epoxy groups of ABS-*g*-GMA copolymer; these are listed in Scheme 1. Reactions 1 and 2 belong to compatibilization reactions, which postulate the formation of PLA-*co*-ABS copolymers at the blend interface. The PLA-*co*-ABS copolymer, acting as compatibilizer, can increase interfacial strengths and reduce the disperse-phase coalescence rate through steric repulsion. Simultaneously, the disperse-phase breakup rate increases through lowered interfacial tension. These factors result in a finer distribution of the disperse phase and response for the better morphological properties of the PLA/ABS-*g*-GMA blend (shown later in the morphological properties part). Reactions 3 and 4 present the crosslinking reactions proposed to occur in PLA/ABS-*g*-GMA blends. Reaction 3 involves the secondary hydroxyl groups present on the copolymers of PLA-*co*-ABS formed at the interface, and this reaction takes place in the disperse phase itself. Reaction 4 is based on the bifunctionality of the PLA matrix, as each PLA contains two functional groups that can react with the epoxy groups. In contrast with reaction 3, this crosslinking reaction occurs mainly at the interface. The proposed crosslinking reactions will interfere with the phase morphology formation.

Figures 3 and 4 show the evolution of torque and temperature versus time for the PLA/ABS and PLA/ABS-*g*-GMA blends containing different GMA contents in the ABS-*g*-GMA copolymer. It can be seen from Figure 3 that, compared to the PLA/ABS-*g*-GMA blend, the PLA/ABS blend had the lowest

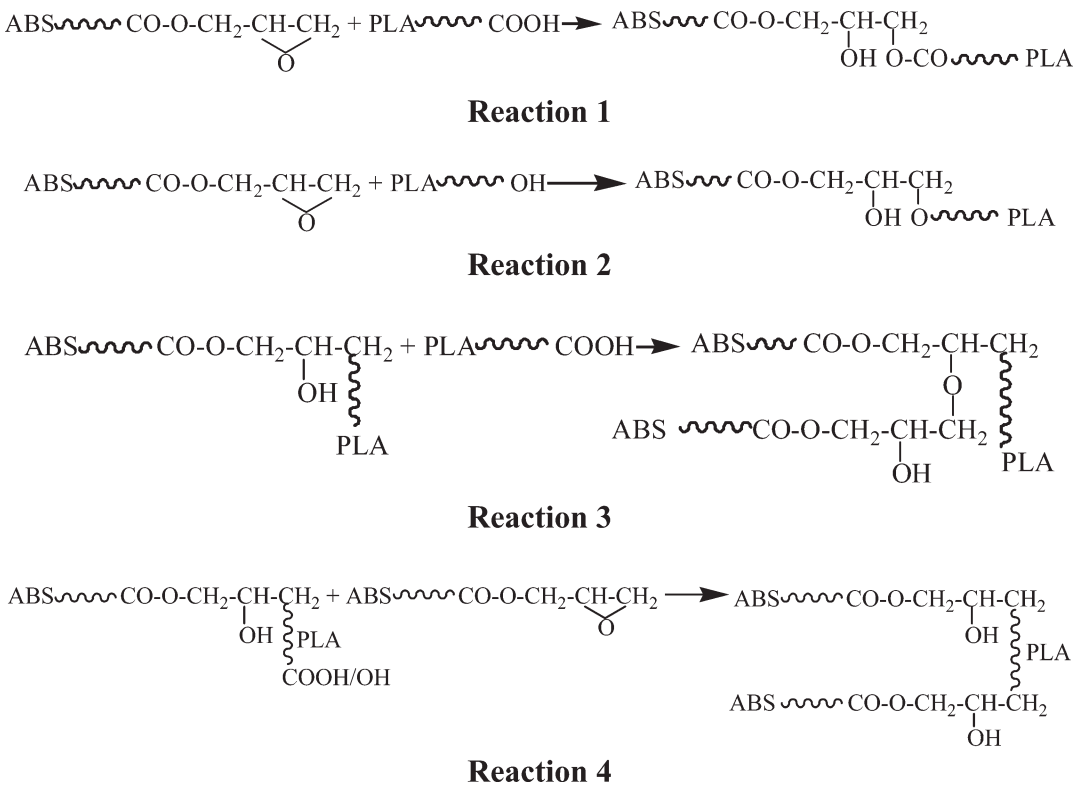

Scheme 1 Reactions in PLA/ABS-*g*-GMA blends.

torque value because there was no chemical reaction between PLA and ABS. For the PLA/ABS-*g*-GMA blends, the torque value of these blends increased with the increase of GMA content in the ABS-*g*-GMA copolymer; this further identified the reactions between the epoxy group of GMA and the functional group of PLA.

Figure 4 illustrates the relation between the actual temperature in the mixer and mixing time for the PLA blends. The actual temperature in the mixer increased rapidly during a short time interval, and it reached 184°C for the PLA/ABS blend; this was higher than the setting temperature 180°C because of viscous heating of the polymer. As for the PLA/ABS-*g*-GMA blends, the temperature in the mixer got higher. This was due to the viscous heating of the highly viscous PLA-*co*-ABS copolymer or cross-linking products.

Morphological properties

SEM micrographs of the cryofractured surfaces of the PLA blends are shown in Figure 5. As can be seen from Figure 5(a), obvious agglomeration

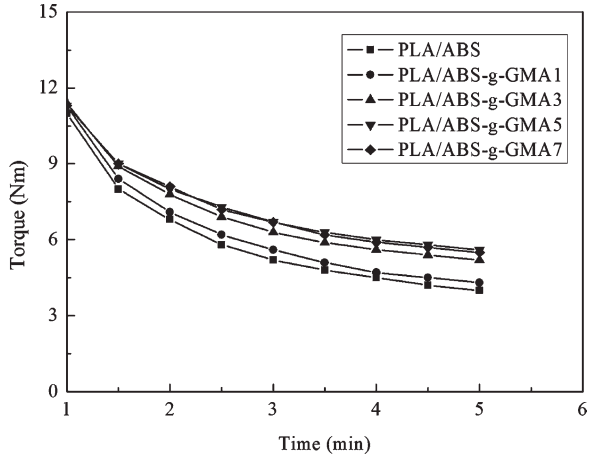

Figure 3 Evolution of the torque with time in the PLA/ABS-*g*-GMA blends.

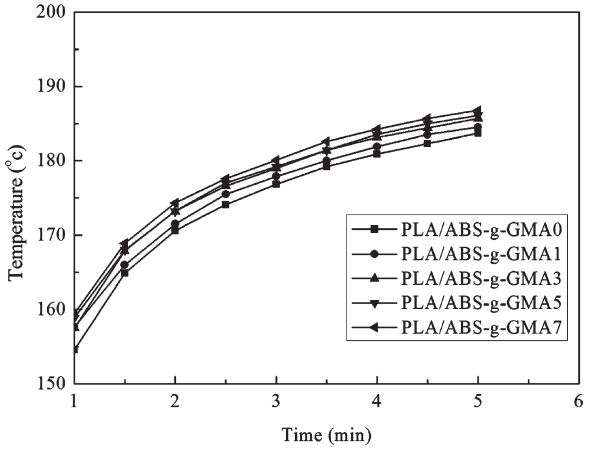

Figure 4 Evolution of the temperature with time in the PLA/ABS-*g*-GMA blends.

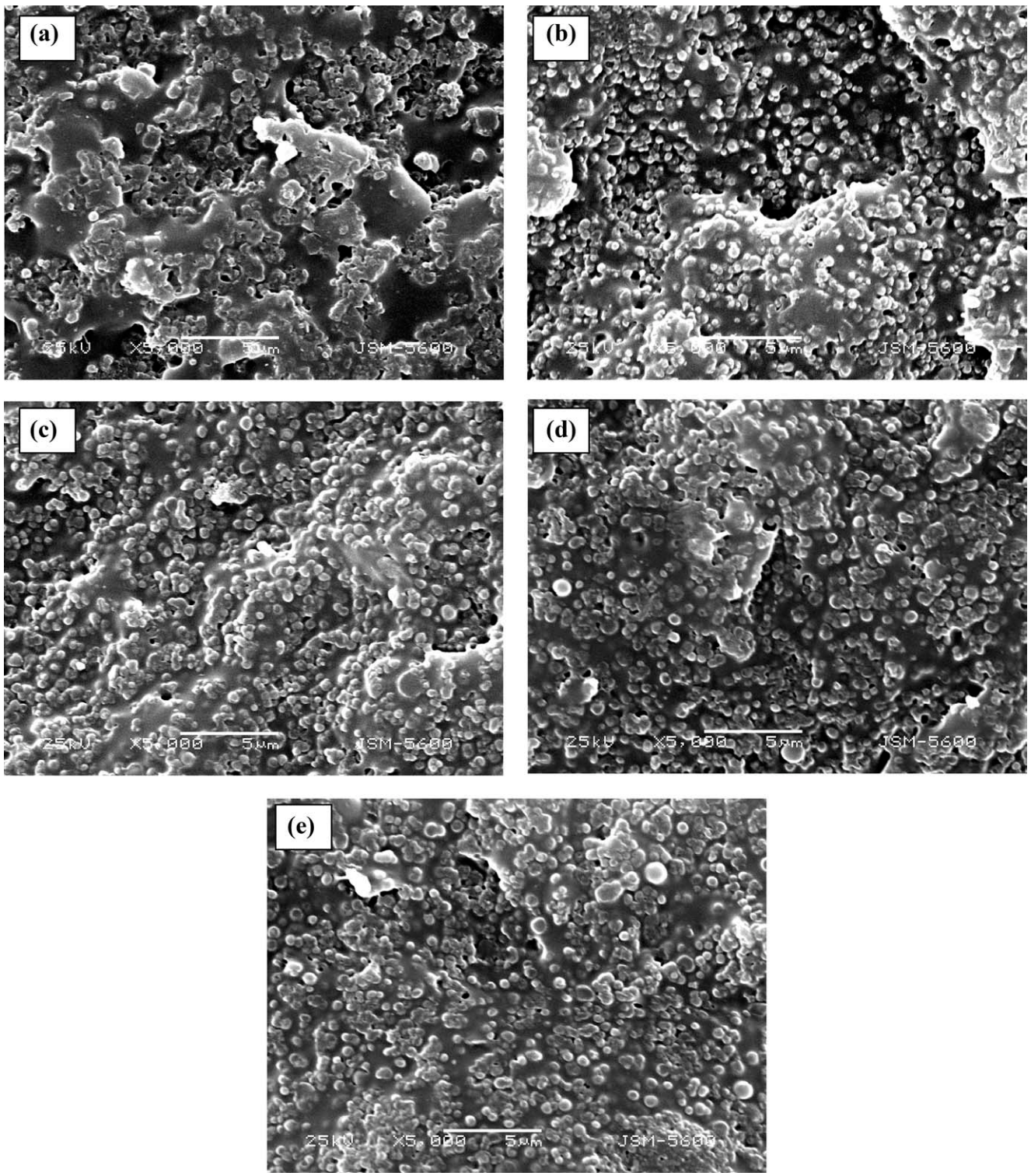

Figure 5 Morphology of PLA/ABS-*g*-GMA blends with different GMA contents. (a) PLA/ABS, (b) PLA/ABS-*g*-GMA1, (c) PLA/ABS-*g*-GMA3, (d) PLA/ABS-*g*-GMA5, (e) PLA/ABS-*g*-GMA7.

occurred for ABS particles and formed a big phase size because of the high interfacial tension between PLA and ABS; this indicated the poor miscibility of the two phases. Figure 5(b–e) show the PLA/ABS-*g*-GMA blends. Compared with the PLA/ABS blend, the introduction of GMA onto ABS modified the phase morphology significantly. The coalescence of ABS particles was suppressed. However, the phase morphology showed some difference because of the different GMA contents in the ABS-*g*-GMA particles. The PLA/ABS-*g*-GMA1 blend showed a much better disperse phase morphology, and most

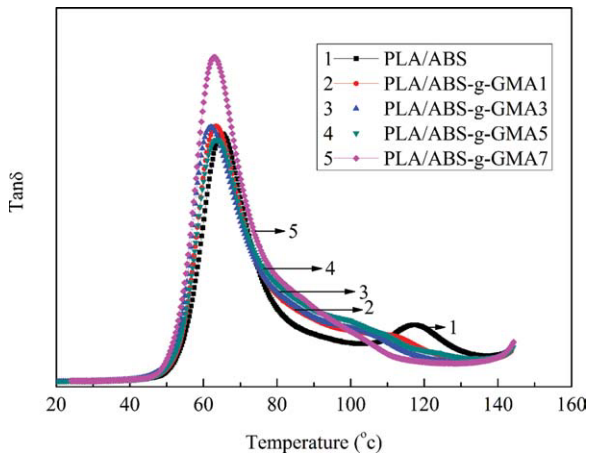

Figure 6 Relationship between tan δ and the temperature for PLA/ABS-*g*-GMA blends with different GMA contents. [Color figure can be viewed in the online issue, which is available at wileyonlinelibrary.com.]

of the ABS-*g*-GMA particles dispersed in the PLA matrix uniformly; this proved the compatibilization effect of the PLA-*co*-ABS copolymers due to the compatibilization reactions between PLA and ABS-*g*-GMA. The PLA-*co*-ABS copolymers at the interface decreased the interfacial tension and prohibited the agglomeration of the dispersed phase. However, with the increase of GMA content, the agglomeration of part of the ABS particles took place; this can be seen in Figure 5(c–e). The change of the PLA/ABS-*g*-GMA phase morphology was in the crosslinking reactions between PLA and ABS-*g*-GMA, as discussed in the chemical reactions analysis part. The formation of PLA-*co*-ABS and the subsequent crosslinking of the ABS-*g*-GMA took place more rapidly in case of PLA/ABS-*g*-GMA blends containing higher GMA contents and induced the obvious agglomeration of ABS-*g*-GMA particles because of the crosslinking reactions.

DMA

DMA was used to analyze the miscibility and modulus changes of the PLA blends. As shown from the tan δ and temperature relation curves of Figure 6, the PLA/ABS blend showed two glass transitions, one for the PLA phase at about 65°C and the other for SAN phase at about 117°C (the SAN copolymer was the shell phase of ABS particles). DMA indicated that PLA and ABS were not thermodynamically miscible. However, with the introduction of GMA onto ABS particles, the miscibility between the PLA and ABS blends improved significantly. As shown in Figure 6, the tan δ peak of the PLA phase shifted to lower temperature to some degree, although the change was small, which was different from some investigations because, in most cases, the improvement of miscibility induces the glass-transition temperature shift together. The tan δ peak of the SAN phase changed wide and shifted to lower temperature obviously, and with the increase of GMA content in ABS-*g*-GMA particles, the glass transition of the SAN phase became obscure; this proved that the miscibility between PLA and ABS-*g*-GMA improved because of the compatibilization reactions.

Figure 7 shows the storage modulus (E') and temperature relation curves of the PLA blends. The peaks near 112°C for the PLA blend E' curves in Figure 7 are cold crystallization peaks of the PLA phase, which have been found in other articles.[30,31] As can be seen from Figure 7, with the increase of GMA content in the ABS-*g*-GMA particles, the cold crystallization peak of the PLA phase in the PLA/ABS-*g*-GMA blends became poor; this indicates that the crystallization ability of PLA was suppressed because of the chemical reactions in the PLA/ABS-*g*-GMA blends.

The E' of the blends dropped abruptly near the glass-transition temperature of the PLA phase, and it could be found that when the temperature was lower than the glass-transition temperature of the PLA phase, the E' of the blends decreased with the increase of GMA content in ABS-*g*-GMA. The E' decrease of the PLA blends with the increase of GMA content was in the chemical reactions between the epoxy groups of ABS-*g*-GMA and the end carboxyl or hydroxyl groups of PLA, which increased the viscosity of the blends and suppressed the movement of PLA chains. So, the crystallization of the PLA phase became difficult, and the crystallization degree of PLA decreased; this induced the decrease of the PLA blends' E'.

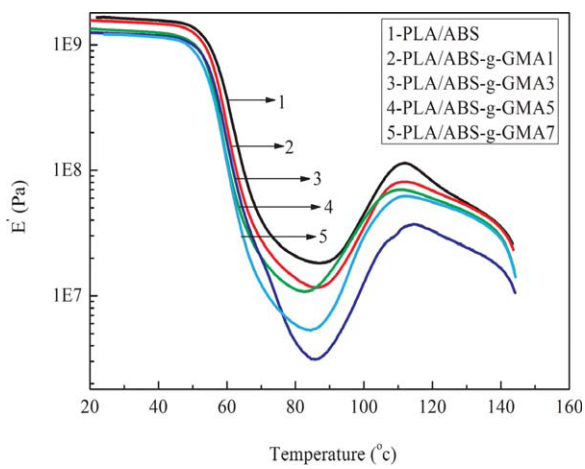

Figure 7 Relationship between E' and the temperature for PLA/ABS-*g*-GMA blends with different GMA contents. [Color figure can be viewed in the online issue, which is available at wileyonlinelibrary.com.]

Mechanical properties

Figure 8 shows the notched Izod impact strength and elongation at break of PLA blends; this indicated the toughness improvement of PLA with the addition of ABS and ABS-*g*-GMA particles. The notched impact strength of pure PLA was about 20 J/m, whereas the PLA/ABS blend possessed a notched impact strength of about 50 J/m. Although ABS improved the toughness of PLA by a factor of 2.5, which represented a moderate improvement, the blend still fractured in brittle mode. The toughness of PLA improved significantly with the addition of ABS-*g*-GMA. As for the PLA/ABS-*g*-GMA1 blend, the notched impact strength of 540 J/m was achieved; this was 27 times that of pure PLA and the blend fractures in ductile mode. The obvious improvement of toughness for PLA/ABS-*g*-GMA1 blend was in the compatibilization reactions, which modified the phase morphology of the blend, as shown in Figure 5(a), and induced the improvement of the toughness. However, with the increase of GMA content in the ABS-*g*-GMA particles, the notched impact strength of the blends decreased again because of the crosslinking reactions. The elongation at break of the blends showed similar changes with the notched impact strength. So, in this study, a 1 wt % GMA content in the ABS-*g*-GMA particles was sufficient to satisfy the compatibilization and to obtain toughened PLA blends. Higher GMA content was not beneficial to the properties modification of PLA because of the crosslinking reactions.

The toughness improvement of PLA in these results was compared with other reports. POE-*g*-GMA was used to toughen PLA by Su et al.[29] The impact strength increased from 4.0 ± 0.7 kJ/m^2 for PLA to 46.1 ± 5.6 kJ/m^2 for PLA/POE-*g*-GMA blends when the content of POE-*g*-GMA was 30 wt %. EGMA was used by Oyama[28] to modify the toughness of PLA. However, the toughness was not improved significantly before annealing for the blend with 20 wt % EGMA addition. The melt blending of PLA and poly(ether) urethane elastomer was performed in an effort to toughen PLA by Li and Shimizu.[31] It was found that the impact strength was changed from 64 J/m^2 for neat PLA to 315 J/m^2 for the PLA/poly(ether) urethane 70/30 blends. ABS is another important toughener of PLA. Li and Shimizu[30] used an SAN–GMA copolymer as a compatibilizer and ethyltriphenyl phosphonium bromide (ETPB) as the catalyst for poly(L-lactide) (PLLA)/ABS blends. The impact strength of PLLA improved from 69.7 to 123.9 kJ/m^2 for the PLLA/ABS/SAN–GMA/ETPB 70/30/5/0.02 phr blend.

From the reports, it was found that the ABS-*g*-GMA core–shell particles used in this study showed a much higher toughening efficiency than the reported elastomers. The reason may have been in the higher toughening ability of the PB particles as the rubber phase of the ABS-*g*-GMA copolymer. As for the different toughness improvement of the PLA/ABS-*g*-GMA blends from the PLLA/ABS/SAN–GMA/ETPB blends investigated by Li and Shimizu,[30] there are two possible reasons. One lies in the different ABS used by the studies. The ABS-*g*-GMA particle used in our study was a core–shell copolymer. The core was the PB phase, and the shell phase was the SAN–GMA copolymer. The ABS-*g*-GMA particles had a higher rubber component of 60 wt %, which displayed a higher toughening ability. Second, the GMA was grafted onto the shell phase of ABS, which was located in the interface between ABS and PLA, so the interfacial reactions between the two phases were much easier. The two reasons induced the higher toughening efficiency of ABS-*g*-GMA for the PLA matrix.

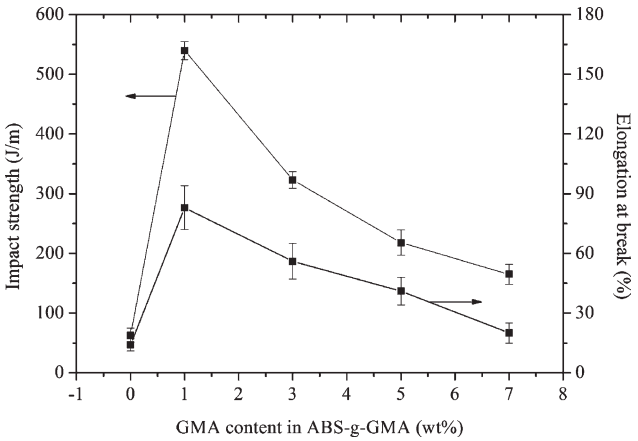

Figure 8 Mechanical properties of PLA/ABS-*g*-GMA blends with different GMA contents.

CONCLUSIONS

ABS-*g*-GMA was synthesized by emulsion polymerization. FTIR results show that the GMA monomers grafted onto the polybutylene phase of the ABS particles. The epoxy-functionalized ABS-*g*-GMA particles were used to improve the toughness of PLA. In the PLA/ABS-*g*-GMA blends, compatibilization and crosslinking reactions took place simultaneously between the epoxy groups of ABS-*g*-GMA and the carboxyl or hydroxyl end groups of PLA. The reactions were affected by the GMA content in ABS-*g*-GMA particles. DMA tests showed improved miscibility between PLA and ABS with the introduction of GMA. The decrease of E' of PLA/ABS-*g*-GMA with the increase of GMA content was due to the decrease of the crystallization ability of PLA. Morphological and mechanical tests showed that a 1 wt % GMA content in ABS-*g*-GMA particles was sufficient to satisfy the compatibilization and to obtain toughened PLA blends.

References

1. Grijpma, D. W.; Pennings, A. J. Macromol Chem Phys 1994, 195, 1649.
2. Hiljanen Vainio, M.; Karjalainen, T.; Seppala, J. J Appl Polym Sci 1996, 59, 1281.
3. Ruckenstein, E.; Yuan, Y. J Appl Polym Sci 1998, 69, 1429.
4. Baiardo, M.; Frisoni, G.; Scandola, M.; Rimelen, M.; Lips, D.; Ruffieux, K.; Wintermantel, E. J Appl Polym Sci 2003, 90, 1731.
5. Jacobsen, S.; Fritz, H. G. Polym Eng Sci 1999, 39, 1303.
6. Labrecque, L. V.; Kumar, R. A.; Dave, V.; Gross, R. A.; McCarthy, S. P. J Appl Polym Sci 1997, 66, 1507.
7. Martin, O.; Averous, L. Polymer 2001, 42, 6209.
8. Anderson, K. S.; Lim, S. H.; Hillmyer, M. A. J Appl Polym Sci 2003, 89, 3757.
9. Wang, Y.; Hillmyer, M. A. J Polym Sci Part A: Polym Chem 2001, 39, 2755.
10. Tams, J.; Joziasse, C. A. P.; Bos, R. R. M.; Rozema, F. R.; Grijpma, D. W.; Pennings, A. J. Biomaterials 1995, 16, 1409.
11. McCarthy, S. P.; Ranganthan, A.; Ma, W. Macromol Symp 1999, 144, 63.
12. Grijpma, D. W.; Van Hofslot, R. D. A.; Super, H.; Nijenhuis, A. J.; Pennings, A. J. Polym Eng Sci 1994, 34, 1674.
13. Hiljanen Vainio, M.; Varpomaa, P.; Seppala, J.; Tormala, P. Macromol Chem Phys 1996, 197, 1503.
14. Nijenhuis, A. J.; Colstee, E.; Grijpma, D. W.; Pennings, A. J. Polymer 1996, 37, 5849.
15. Kim, K.; Chin, I.; Yoon, J. S.; Choi, H. J.; Lee, D. C.; Lee, K. H. J Appl Polym Sci 2001, 82, 3618.
16. Focarete, M. L.; Scandola, M.; Dobrzynski, P.; Kowalczuk, M. Macromolecules 2002, 35, 8472.
17. Tsuji, H.; Ikada, Y. J Appl Polym Sci 1996, 60, 2367.
18. Wang, L.; Ma, W.; Gross, R. A.; McCarthy, S. P. Polym Degrad Stab 1998, 59, 161.
19. Joziasse, C. A. P.; Topp, M. D. C.; Veenstra, H.; Grijpma, D. W.; Pennings, A. J. Polym Bull 1994, 33, 599.
20. Hiljanen-Vainio, M.; Kylma, J.; Hiltunen, K.; Seppala, J. V. J Appl Polym Sci 1997, 63, 1335.
21. Ruckenstein, E.; Yuan, Y. Polym Bull 1998, 40, 485.
22. Creton, C.; Kramer, E. J.; Hui, C. Y.; Brown, H. R. Macromolecules 1992, 25, 3075.
23. Kim, J. K.; Lee, H. Polymer 1996, 37, 305.
24. Jeon, H. K.; Kim, J. K. Polymer 1998, 39, 6227.
25. Cecere, A.; Greco, R.; Ragosta, G.; Scarinzi, G.; Taglialatela, A. Polymer 1990, 31, 1239.
26. Sun, Y. J.; Hu, G. H.; Lambla, M.; Kotlar, H. K. Polymer 1996, 37, 4119.
27. Hu, G. H.; Sun, Y. J.; Lambla, M. Polym Eng Sci 1996, 36, 676.
28. Oyama, H. T. Polymer 2009, 50, 747.
29. Su, Z.; Li, Q.; Liu, Y.; Hu, G.; Wu, C. Eur Polym J 2009, 45, 2428.
30. Li, Y.; Shimizu, H. Eur Polym J 2009, 45, 738.
31. Li, Y.; Shimizu, H. Macromol Biosci 2007, 7, 921.